Fusion Engineering and Design 88 (2013) 529–532

Contents lists available at ScienceDirect

Fusion Engineering and Design

journal homepage: www.elsevier.com/locate/fusengdes

# Numerical modeling of 3D halo current path in ITER structures

Paolo Bettini [a], Nicolò Marconato [a], Maurizio Furno Palumbo [a], Simone Peruzzo [a], Ruben Specogna [b,*], Raffaele Albanese [c], Guglielmo Rubinacci [c], Salvatore Ventre [c], Fabio Villone [c]

[a] Consorzio RFX, EURATOM-ENEA Association, C.so Stati Uniti 4, 35127 Padova, Italy
[b] DIEGM, Università di Udine, Via delle Scienze, 208, 33100 Udine, Italy
[c] Consorzio CREATE, EURATOM-ENEA Association, Via Claudio 21, 80125 Napoli, Italy

HIGHLIGHTS

- Two numerical codes for the evaluation of halo currents in 3D structures are presented.
- A simplified plasma model is adopted to provide the input (halo current injected into the FW).
- Two representative test cases of ITER symmetric and asymmetric VDEs have been analyzed.
- The proposed approaches provide results in excellent agreement for both cases.

ARTICLE INFO

*Article history:*
Available online 20 December 2012

*Keywords:*
Halo currents
Numerical modeling
3D passive structures
ITER

ABSTRACT

Disruptions represent one of the main concerns for Tokamak operation, especially in view of fusion reactors, or experimental test reactors, due to the electro-mechanical loads induced by halo and eddy currents. The development of a predictive tool which allows to estimate the magnitude and spatial distribution of the halo current forces is of paramount importance in order to ensure robust vessel and in-vessel component design. With this aim, two numerical codes (CARIDDI, CAFE) have been developed, which allow to calculate the halo current path (resistive distribution) in the passive structures surrounding the plasma. The former is based on an integral formulation for the eddy currents problem particularized to the static case; the latter implements a pair of 3D FEM complementary formulations for the solution of the steady-state current conduction problem. A simplified plasma model is adopted to provide the inputs (halo current injected into the first wall). Two representative test cases (ITER symmetric and asymmetric VDEs) have been selected to cross check the results of the proposed approaches.


## 1. Introduction

Disruptions represent one of the main concerns for Tokamak operation, especially in view of fusion reactors, or experimental test reactors, such as ITER [1]. Halo and eddy currents are the main source of electro-mechanical loads during disruptions. In particular, halo currents contribute to both global vessel loads, which can be extrapolated from disruption database information on halo current fraction and toroidal peaking factor (TPF) [2], and to local in-vessel component loads, which depend on the halo current density and for which less information is available [3,4].

Even though a fully self-consistent physical model for the prediction of the halo current is still not available, due to the complexity of the phenomena involved, the development of a predictive understanding of the magnitude and spatial distribution of the halo current forces is of paramount importance in order to ensure robust vessel and in-vessel component design.

In this work two numerical codes (CARIDDI, CAFE) are presented, which allow to calculate the resistive distribution of the halo current density in the conducting structures surrounding the plasma. CARIDDI and CAFE treat only the passive structures and need input from the plasma side in the form of boundary conditions according to the procedure described in Section 2.

Two representative test cases of ITER vertical displacement events (VDEs) have been selected to asses the performance of the proposed approaches.

## 2. Specification and simulation of VDEs

A description of the VDE loads expected in ITER has been recently published [2], with particular emphasis on the asymmetric VDEs (AVDEs). The proposed approach, based on experimental observations from several existing tokamaks, considers plasma MHD deformations during VDEs associated to dominant kink

* Corresponding author. Tel.: +39 0432558037.
*E-mail address:* ruben.specogna@uniud.it (R. Specogna).

0920-3796/$ – see front matter © 2012 Elsevier B.V. All rights reserved.
http://dx.doi.org/10.1016/j.fusengdes.2012.11.017

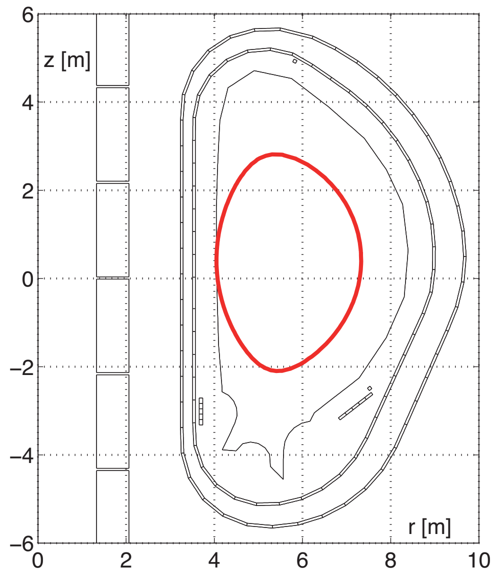


**Fig. 1.** Sample ITER equilibrium computed by CREATE-NL. Main plasma parameters: $I_p$ = 5.4 MA, $\beta_p$ = 0.06, $\ell_i$ = 1.04.

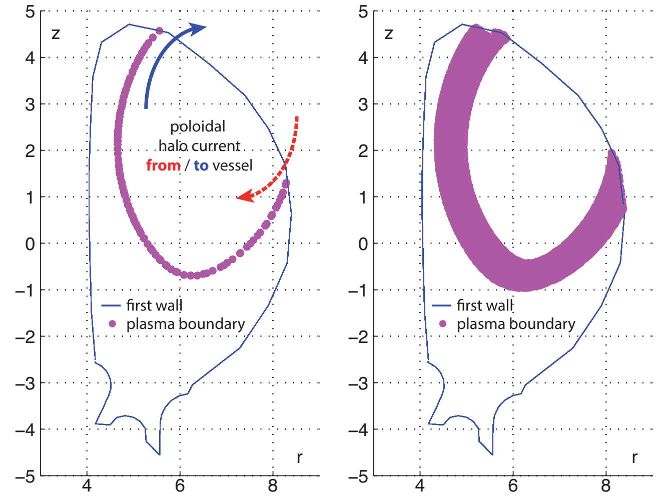


**Fig. 2.** Projection of plasma boundary onto a poloidal plane for a symmetric VDE (left) and an AVDE (right).

modes $m = 1$, $n = 1$, which correlate with the largest asymmetric electromagnetic loads on the mechanical structures. In this study a simplified plasma model is adopted which can give rise to any n-component of the halo current injected into the FW at given values of the radial/vertical coordinates of the fixed frame by means of spatial transformations (rigid motion and expansion/contraction) of low beta axi-symmetric equilibria computed with CREATE-NL code [8].

In this way, since the plasma and all the other currents and fields are translated, rotated or expanded and remain axi-symmetric in their coordinate system, the following important properties are kept

- plasma core: $\mathbf{J} \times \mathbf{B} = \nabla p$
- halo region: $\mathbf{J} \times \mathbf{B} = 0 \Rightarrow J \parallel B$
- $\nabla \cdot \mathbf{B} = 0 \quad \& \quad \nabla \cdot \mathbf{J} = 0 \quad \& \quad \nabla \times \mathbf{B} = \mu_0 \mathbf{J}$

Starting from the equilibrium shown in Fig. 1, two configurations have been selected as representative test cases: a symmetric VDE and an AVDE. The parameters adopted to obtain the configurations are reported in Table 1, while Fig. 2 shows the results of the plasma boundary projected onto a poloidal plane; for the VDE the boundary and the region of interaction with the FW are constant whereas for the AVDE they vary along the toroidal direction.

## 3. Numerical codes

Two numerical codes (CARIDDI, CAFE) have been developed which allow to compute the resistive distribution of the halo current density in the conducting structures surrounding the plasma. The former, based on an integral formulation, is described in Section 3.1; the latter, which implements a pair of complementary formulations, is described in Section 3.2.

**Table 1**
Perturbation parameters adopted to simulate a symmetric VDE and an AVDE; displacement ($\triangle x$, $\triangle y$, $\triangle z$), tilts around $x$-axis ($\alpha$) and $y$-axis ($\beta$), expansion coefficient ($\kappa$).

| Case | $\triangle x$ (m) | $\triangle y$ (m) | $\triangle z$ (m) | $\alpha$ (°) | $\beta$ (°) | $\kappa$ |
|---|---|---|---|---|---|---|
| VDE | 0 | 0 | +1.45 | 0 | 0 | 1.15 |
| AVDE | 0.25 | 0 | +1.45 | 2.5 | 0 | 1.15 |

### 3.1. Integral formulation – CARIDDI

The three-dimensional conducting structure $V_c$ is described using the integral formulation for the eddy currents problem presented in [6], particularized to the static case. By imposing Ohm's law on $V_c$ in weak form, we have

$$\int_{V_c} \nabla\phi \cdot \mathbf{w}\, dV + \int_{V_c} \eta \mathbf{J} \cdot \mathbf{w}\, dV = 0 \qquad \forall \mathbf{w} \tag{1}$$

where $\phi$ is the electric scalar potential, $\mathbf{w}$ is a suitable weight function, $\eta$ is the resistivity tensor and $\mathbf{J}$ is the current density in $V_c$, whose solenoidality is imposed introducing the electric vector potential $\mathbf{T}$, such that $\mathbf{J} = \nabla \times \mathbf{T}$, with the two-component gauge. Giving a finite elements discretization of $V_c$, $\mathbf{T}$ is expanded in terms of edge elements $\mathbf{N}_k$. The gauge is imposed by computing a tree-cotree decomposition of the mesh and retaining only the degrees of freedom (DoF) related to the edges belonging to the cotree, giving rise to $N$ DoFs. Adopting the Galerkin method, (1) becomes

$$\underline{\underline{R}}\,\underline{I} + \underline{\underline{P}}^T\,\underline{V} = 0, \tag{2}$$

where

$$\begin{aligned} R_{ij} &= \int_{V_c} \nabla \times \mathbf{N}_i \cdot \eta \nabla \times \mathbf{N}_j\, dV \\ P_{kh} &= -\int_{\Sigma_k} \nabla \times \mathbf{N}_h \cdot \hat{\mathbf{n}}\, dV \end{aligned} \tag{3}$$

where $\underline{I} = \{I_k\}_{k=1,\ldots,N}$ is the set of discrete DoF and $\underline{V} = \{V_k\}_{k=1,\ldots,M}$ is the set of voltages on the $M$ boundary facets of the mesh $\Sigma_k$, whose normal is $\hat{\mathbf{n}}$.

In order to find the unknown voltages $\underline{V}$, (2) must be complemented by the following constraints

$$\underline{\underline{P}}\,\underline{I} = \underline{I}_{ass} \tag{4}$$

where $\underline{I}_{ass}$ is the vector of $M$ assigned currents through each boundary facet of the mesh. Such value must be equal to the plasma halo current imposed through each mesh facet (zero if no current is flowing through it). The constraints (4) are imposed with the same approach described in [7], i.e. with the following decomposition:

$$\underline{I} = \underline{I}_0 + \underline{\underline{Z}}\,\underline{I}_{add}, \tag{5}$$

where $\underline{I}_0 = \underline{\underline{P}}^+ \underline{I}_{ass}$ ($\underline{\underline{P}}^+$ is the Moore–Penrose pseudoinverse of $\underline{\underline{P}}$) and $\underline{\underline{Z}}$ is a basis for the null space of $\underline{\underline{P}}$. By multiplying (2) by $\underline{\underline{Z}}^T$, exploiting the fact that $\underline{\underline{Z}}^T\,\underline{\underline{P}}^T\,\underline{V} = (\underline{V}^T\,\underline{\underline{P}}\,\underline{\underline{Z}})^T = 0$, we have

$$\underline{\underline{Z}}^T\,\underline{\underline{R}}\,\underline{\underline{Z}}\,\underline{I}_{add} = -\underline{\underline{Z}}^T\,\underline{\underline{R}}\,\underline{I}_0 \tag{6}$$

The resulting system of equations (6) is solved using an iterative solver (ICCG), taking into account the fact that matrix $\underline{\underline{R}}$ in (3) is very sparse.

### 3.2. Complementary formulations – CAFE

CAFE uses the standard FEM formulation **V** based on the electric scalar potential together with an original formulation **T** that employs the electric vector potential [9]. The advantage of using two formulations arising from complementary potentials is that the constitutive error [10] is minimized and an accurate solution may be obtained as the mean between the ones produced by the pair of complementary formulations. Nonetheless, complementarity usually is not exploited in practice because of theoretical issues arising in the vector potential formulation that originate from the fact that the computational domain is not simply connected.

The computational domain is covered by a hexahedral mesh whose incidences are encoded in the *cell complex* $\mathcal{K}$ represented by the standard incidence matrices **G**, **C** and **D**. A dual barycentric complex $\tilde{\mathcal{K}}$ is obtained from $\mathcal{K}$ by using the *barycentric subdivision* [9]. The matrices $\tilde{\mathbf{G}} = \mathbf{D}^T$, $\tilde{\mathbf{C}} = \mathbf{C}^T$ and $\tilde{\mathbf{D}} = -\mathbf{G}^T$ represent the incidence matrices of $\tilde{\mathcal{K}}$. In order to formulate the problem by using the vector potential formulation, an array of voltages $\tilde{\mathbf{U}}$ on dual edges $\tilde{e}$, an array of currents **I** on faces *f* and an electric vector potential **T** on edges *e* are introduced. The vector potential defined with

$$\mathbf{I} = \mathbf{I}_s + \mathbf{CT} + \sum_{i=1}^{N} I_g^i \mathbf{\Pi}^i \tag{7}$$

verifies the discrete continuity law $\mathbf{DI} = \mathbf{0}$, where the $\{\mathbf{\Pi}^i\}$ is a set of *thick links* [9], $\{I_g^i\}_{i=1}^n$ is the corresponding set of independent currents and $\mathbf{I}_s$ is the prescribed current. $\mathbf{I}_s$ on mesh faces belonging to $\partial\mathcal{K}$ is set to the plasma halo current imposed through them. The values on internal faces are found iteratively by imposing $\mathbf{DI}_s = 0$ with a spanning tree technique [9]. A similar constraint is imposed implicitly in CARIDDI by Eq. (5). Concerning boundary conditions, **T** is set to zero for all edges $e \in \partial\mathcal{K}$. The *resistivity matrix* **R** relates the currents **I** to voltages $\tilde{\mathbf{U}}$ with $\tilde{\mathbf{U}} = \mathbf{RI}$. Concerning the construction of **R**, an efficient solution is to use the piecewise-uniform edge and face vector basis functions defined in [11] for general polyhedra.

By combining the Faraday's discrete law $\mathbf{C}^T\tilde{\mathbf{U}} = \mathbf{0}$ with (7) and Ohm's law an algebraic equation is obtained for each dual face

$$\mathbf{C}^T\mathbf{RCT} + \sum_{j=1}^{N} (\mathbf{C}^T\mathbf{R}\boldsymbol{\Pi}^j) I_g^j = -\mathbf{C}^T\mathbf{RI}_s. \tag{8}$$

The final algebraic linear system of equations (8) contains as unknowns also the independent currents $\{I_g^j\}_{j=1}^N$. To get as many equations as the unknowns, a set of *non-local Faraday's laws* [9] has to be written on each thick link as $\boldsymbol{\Pi}^{iT}\tilde{\mathbf{U}} = 0,\ i \in \{1, \ldots, N\}$ and expanded as

$$(\boldsymbol{\Pi}^{iT}\mathbf{RC})\mathbf{T} + \sum_{j=1}^{N} (\boldsymbol{\Pi}^{iT}\mathbf{R}\mathbf{\Pi}^j) I_g^j = -\boldsymbol{\Pi}^{iT}\mathbf{RI}_s. \tag{9}$$

The final algebraic linear system (sparse, symmetric and singular) is solved by an iterative solver using an *ungauged* technique.

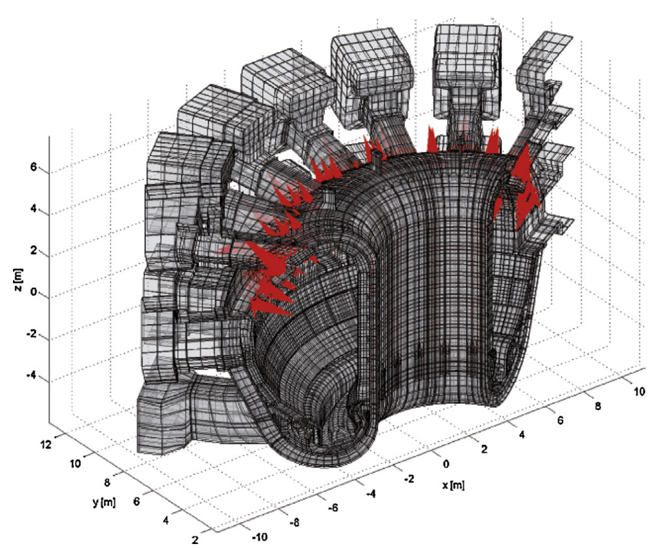


**Fig. 3.** Solution of the VDE test case computed by CARIDDI: halo current density vectors on a quarter of the model.

## 4. Results

The assessment of the performance of the proposed approaches is based on the following steps:

- Development of a detailed 3D model of the relevant ITER structures (including vessel, port extensions, blanket modules, divertor): the mesh adopted consists of ≈240, 000 hexahedra.
- Identification of the mesh elements facing the plasma, where the input current is prescribed by means of the code described in Section 2.
- Evaluation of the resistive distribution of the currents inside the 3D structures by means of the numerical codes described in Section 3.
- Comparison of the results in terms of current density components $(J_x, J_y, J_z)$ in each mesh element.

As for the symmetric VDE test case, the solution computed by CARIDDI is presented in Fig. 3 in terms of halo current density vectors on a quarter of the model. In Fig. 4a comparison of the results of

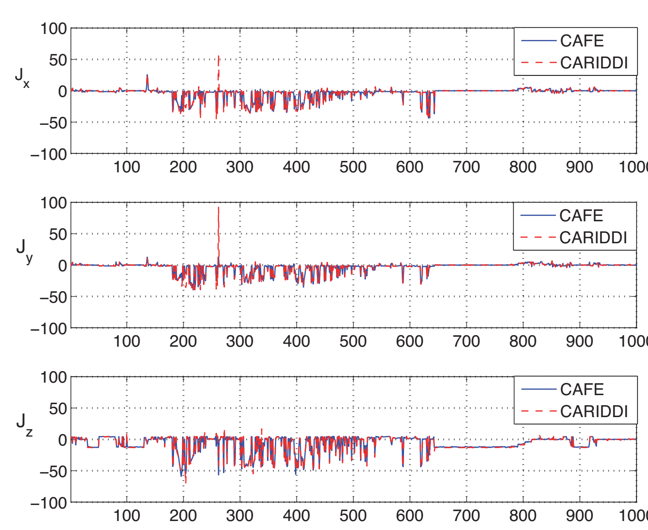


**Fig. 4.** Cross-check of the results for the symmetric VDE: halo current density ($J_x$, $J_y$, $J_z$ [kA/m$^2$]) on a subset of the mesh.

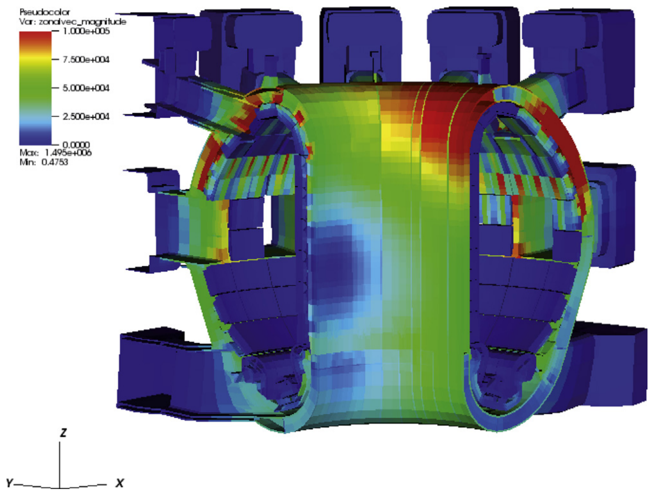


**Fig. 5.** Solution of the AVDE test case computed by CAFE: halo current density magnitude (0–100 kA) on a quarter of the model.

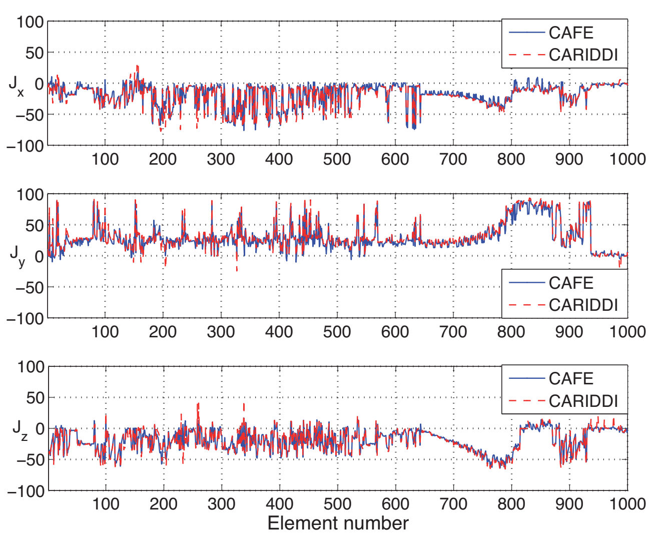


**Fig. 6.** Cross-check of the results for the AVDE: halo current density components ($J_x, J_y, J_z$ [kA/m$^2$]) on a subset of the mesh.

the two numerical codes[1] is presented in terms of halo current density components on a subset of the full model in correspondence with the main interaction region. The agreement is very good for all the components with a RMS discrepancy between the two solutions below 0.1% with respect to the maximum current density value.

As for the AVDE test case, the solution computed by CAFE is presented in Fig. 5 in terms of halo current density magnitude on a quarter of the model. In Fig. 6a comparison of the results of the two numerical codes is presented in terms of halo current density components on a subset of the full model in correspondence with the main interaction region. Also in this case the agreement is very good for all the components with a RMS discrepancy between the two solutions below 0.2% with respect to the maximum current density value.

## 5. Conclusions

A description and cross validation of two numerical codes for the evaluation of the resistive distribution of the halo current density in 3D conducting structures has been presented. Two representative test cases of ITER symmetric and asymmetric VDEs have been selected to asses the performance of the proposed approaches which provide results in excellent agreement.

## Acknowledgements

This work was supported in part by Italian MIUR under PRIN grant #2008E7J7A3. The views and opinions expressed herein do not necessarily reflect those of F4E, nor those of the ITER Organization.

## References

[1] T.C. Hender, et al., Nuclear Fusion 22 (8) (2007) 1015.
[2] C. Bachmann, et al., Fusion Engineering and Design 86 (2011) 1915.
[3] V. Riccardo, et al., Plasma Physics and Controlled Fusion 46 (2004) 925.
[4] G. Pautasso, et al., Nuclear Fusion 51 (2011) 043010.
[6] R. Albanese, G. Rubinacci, IEE Proceedings 135A (5) (1988) 457.
[7] R. Albanese, G. Rubinacci, F. Villone, Journal of Computational Physics 152 (1999) 756.
[8] R. Albanese, et al., Fusion Engineering and Design 66–68 (2003) 715.
[9] R. Specogna, International Journal for Numerical Methods in Engineering 86 (2011) 1041.
[10] J.A.H. Rikabi, IEEE Transactions on Magnetics 29 (1993) 98.
[11] L. Codecasa, R. Specogna, F. Trevisan, Journal of Computational Physics 229 (2010) 7401.

[1] Concerning the results of CAFE code, only the output of the V formulation are displayed, being the results from the **T** formulation very close to the ones obtained by CARIDDI.